003455

PHYSICAL REVIEW B, VOLUME 65, 235431

AgO investigated by photoelectron spectroscopy: Evidence for mixed valence

M. Bielmann,[1] P. Schwaller,[2] P. Ruffieux,[1] O. Gröning,[2] L. Schlapbach,[1] and P. Gröning[1]
[1]*Physics Department, University of Fribourg, Pérolles, CH-1700 Fribourg, Switzerland*
[2]*Materials Technology Department EMPA Thun, Feuerwerkerstrasse 39, CH-3602 Thun, Switzerland*

(Received 18 February 2002; published 20 June 2002)

We present photoelectron spectroscopy investigations of *in-situ* prepared AgO. The sample was prepared by room temperature oxidation of Ag in an electron cyclotron resonance O_2 plasma. In contrast to other measurements based on *ex situ* prepared AgO powder samples, our investigations show a distinct double peak structure of the O $1s$ signal with a remarkable chemical shift of 2.9 eV between the two O $1s$ components. These two components can not be motivated from a crystallographic point of view as the oxygen sites are all equivalent in the unit cell. We interpret this double peak structure as a characteristic feature of AgO and discuss it in terms of mixed valences.

DOI: 10.1103/PhysRevB.65.235431 PACS number(s): 81.65.Mq, 82.33.Xj, 82.80.Pv

I. INTRODUCTION

Silver oxides have been extensively studied in the past due to their high importance in numerous technical applications. For example, the interaction of silver surfaces with oxygen plays a key role for the silver-catalyzed epoxidation of ethylene[1] and the partial oxidation of methanol to formaldehyde.[2] Silver partially oxidizes the reactants instead of producing pure combustion products. Therefore a detailed knowledge of silver oxide surfaces is important for the understanding of catalytical phenomena. Photoelectron spectroscopy (PES) has proven to be an important tool to study silver oxide surfaces. There exists a wide variety of PES data for the two silver oxides AgO and Ag_2O, dating back as far as to the early days of PES.[3–9] In the literature, theoretical work on the topic can also be found.[10–12]

AgO has a monoclinic structure [Fig. 1(a)] containing two inequivalent silver sites. Ag I is twofold coordinated by oxygen while Ag III is fourfold coordinated by O atoms. All oxygen sites are equivalent. AgO is an n-type semiconductor.[15] Ag_2O [Fig. 1(b)] is cubic with six atoms per unit cell. The oxygen atoms form a bcc lattice and are tetrahedrally coordinated by Ag atoms. The bonding in Ag_2O is primarily ionic with Ag^+ and O^{2-} valences[11] making Ag_2O an insulator with an electronic gap of 1 eV (Ref. 7) as observed by UPS. Much work has been devoted to the investigation of silver oxides, however the identification of the oxygen species from PES spectra remains controversial. To some extent this is due to the fact that many groups base their measurements on powder samples transferred to ultrahigh vacuum (UHV) conditions.[3,8,9] Contaminations due to the contact with ambient atmosphere lead to additional oxygen species, complicating the interpretation considerably. Furthermore, AgO is an unstable oxide: it starts to decompose over 100 °C into Ag_2O which itself decomposes above 300 °C.[9] For Ag_2O, Tjeng *et al.*[7] presented an *in situ* preparation method based on a free radical oxygen source. From their work it is obvious that the elimination of contributions from surface contaminations facilitates the interpretation of the spectra. Farhat *et al.*[14–16] produced AgO by O_2 plasma treatment of Ag films evaporated on quarz crystal microbalance (QCM) crystals, but no measurements of the oxide with PES were performed. The role of the plasma is primarily to bypass the dissociative adsorption step. It has been shown by Outlaw *et al.*[17] that oxygen diffusion into the bulk can be increased by more than an order of magnitude if the gas is dissociated in a plasma. In this paper we will, to our knowledge for the first time, present PES data of *in situ* prepared AgO by room temperature oxidation in an electron cyclotron resonance (ECR) O_2 plasma. The measurements reveal a distinct double peak structure in the O $1s$ signal, which we relate to a mixed valency on the oxygen sites.

II. EXPERIMENT

All experiments were performed in a modified Omicron photoelectron spectrometer equipped with an EA 125 HR electron analyzer and an electron cyclotron resonance (ECR) plasma chamber with 2.45 GHz microwave source. The base pressure of the system is 5×10^{-11} mbar. Untreated Ag single crystal surfaces and plasma-treated surfaces were investigated by low-energy electron diffraction (LEED), x-ray photoelectron spectroscopy (XPS), and ultraviolet photoelectron spectroscopy (UPS). As photon sources we used nonmonochromatized Mg $K\alpha$ x rays (1253.6 eV), monochromatized Al $K\alpha$ x rays (1486.6 eV), and He I radiation (21.2 eV) from a gas discharge lamp. The spectrometer is calibrated to a Au $4f_{7/2}$ binding energy (BE) of 83.8 eV. AgO was produced by an ECR O_2 plasma. Prior to oxidation, Ag single crystal surfaces where sputtered with 1.5 keV Ar^+ ions and annealed at ~800 K until a sharp LEED pattern was obtained and no C or O contaminations could be observed by XPS. The oxidation step was performed applying an O_2 ECR

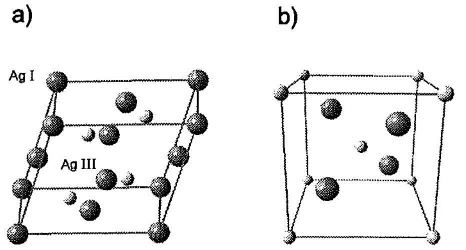

FIG. 1. Unit cells of the AgO and Ag_2O crystal structure (Ref. 13).

0163-1829/2002/65(23)/235431(5)/$20.00 ©2002 The American Physical Society

plasma during 30 min. The gas pressure during the treatment was 3×10^{-2} mbar and the sample was set to ground potential.

The major difference between oxidation under gas flow at elevated temperatures and a ECR plasma treatment is the presence of atomic, excited and ionized atomic species in the plasma. Further, the bulk sample is at RT, but the kinetic energy of the ions striking the surface leads to a local heating of the surface.[22,23] The operation pressure of ECR plasmas is 10^{-4}–10^{-1} mbar. In this pressure range, the electrons and heavy species in the plasma are not in thermodynamical equilibrium, even on a scale in the order of the Debye length λ_D ($\sim$0.1 mm). In such low pressure plasmas the electron temperature T_e is in the range of eV while the temperatures of the heavy species (ions, neutrals) are all in the order of kT ($\sim$25 meV). Therefore such plasmas are generally referred to as cold plasmas.[18] Though the ion temperature T_{ions} is room temperature (RT), a sample inserted into a cold plasma will be struck by ions with a kinetic energy of a few eV. This is due to the fact that a plasma is always positively charged. The excess ions caused by the higher recombination rate of the highly mobile electrons at the container walls compared to the heavy ions ($\langle v_e\rangle \gg \langle v_{\mathrm{ions}}\rangle \leftrightarrow T_e \gg T_{\mathrm{ions}}$) gives rise to the so-called plasma potential. This plasma potential defines the kinetic energy with which the ions strike the surface[19] and depends on the type of plasma as well as the geometry of the setup. Such variations in design can lead to a distinctly different composition of the plasma.[18,19] For our setup, the ion current density is 25 nA/mm^2 and the average O ion energy is about 4 eV for the given parameters as measured by an electrostatic ion energy analyzer.[20]

III. RESULTS AND INTERPRETATION

A. Quartz crystal microbalance

A 50 nm Ag film evaporated *in situ* on a QCM crystal was exposed to the O_2 plasma under identical conditions as the Ag single crystals. The mass uptake during oxidation can be calculated from the dynamically measured change in resonance frequency of the vibrating microbalance crystal. The resulting O /Ag ratio is presented in Fig. 2. After 30 min of oxidation, the O /Ag ratio is 1.05 and therefore an oxidation time of 30 min on the single crystal surfaces was applied. Under the used conditions, AgO layers with well over 1 μm thickness can be prepared. During the plasma treatment, the film changed its color from silver to golden/brownish followed by a dark gray appearance. The brownish color is generally associated with Ag_2O, while the dark gray color is associated with AgO.[21] The same phenomena in color change could also be observed on the single crystal surfaces.

B. X-ray photoelectron spectroscopy

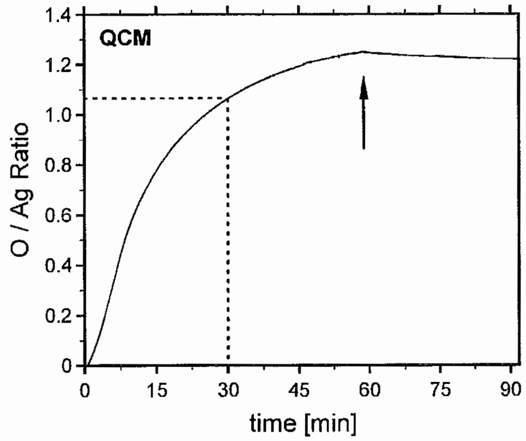

FIG. 2. O/Ag ratio during oxidation of a 50 nm Ag film evaporated on a QCM crystal with gold electrodes. The O/Ag ratio is about 1.05 after 30 min, underlining the conclusion of AgO formation. The arrow indicates the point where the plasma was switched off.

Experiments presented in the following were performed on Ag(110), the most open surface of the low index silver planes. Measurements on the (111) surface revealed identical results in XPS and are therefore not presented. The Ag $3d_{5/2}$ spectra for the clean and the oxidized sample measured with monochromatized Al $K\alpha$, are shown in Fig. 3(a). The corresponding peak positions and peak widths are resumed in Table I. Figure 3(b) shows the O $1s$ spectra after oxidation, exhibiting two distinct components. The lower BE component is centered at 528.6 eV with a FWHM of 0.9 eV. The higher BE component is centered at 531.5 eV with a FWHM of 1.3 eV.

This second peak was not observed by Tjeng *et al.*[7] on Ag_2O. Their spectra exhibit a single O $1s$ signal, at a BE of 528.9 eV. For shorter plasma exposure times, where we assume that predominantly Ag_2O is present, we observe the same O $1s$ signal as Tjeng *et al.*[7] denoted in Table I. But with ongoing oxidation, the lower BE component shifts further down to 528.6 eV and the initially small but present

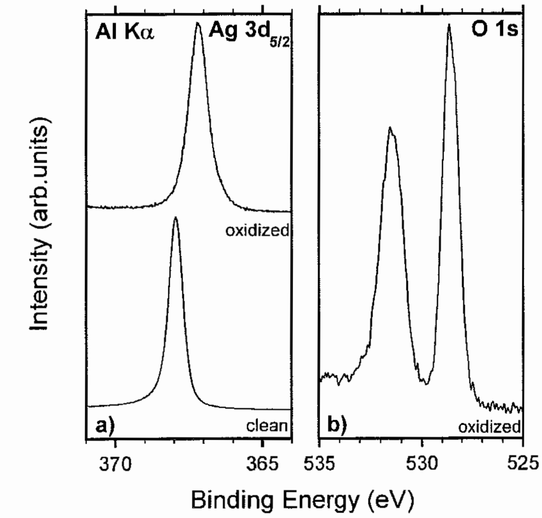

FIG. 3. Ag $3d_{5/2}$ and O $1s$ signals of clean and oxidized Ag(110) by ECR plasma as measured by XPS with monochromatized Al $K\alpha$ radiation. (a) Ag $3d_{5/2}$ signal: the oxidized surface shows a peak shift of -0.8 eV from 368.0 to 367.2 eV and a broadening of 0.2 to 0.76 eV compared to the sputtered and annealed sample. (b) O $1s$ signal: The double peak structure comprises a lower BE component at 528.6 eV with a FWHM of 0.9 eV and a higher BE component of equal intensity at 531.5 eV with a FWHM of 1.3 eV.

TABLE I. Binding energies and peak widths of Ag $3d_{5/2}$ and O $1s$ signals as measured with monochromatized Al $K\alpha$. Values denoted by an asterisk are taken from Tjeng *et al.* (Ref. 7) and were measured with nonmonochromatized Al $K\alpha$.

compound	electron level	BE [eV]	FWHM [eV]
Ag	Ag $3d_{5/2}$	368.0	0.57
AgO	Ag $3d_{5/2}$	367.2	0.76
	O $1s$	528.6	0.9
	O $1s$	531.5	1.3
Ag_2O*	Ag $3d_{5/2}$	367.6	
	O 1s	528.9	1.2

higher BE component grows in intensity until the peak integral of both components are equal. Quantitative analysis of the Ag and O peak intensities taking into account cross sections[24] and analyzer transmission[25] yields an O/Ag ratio of 1.0±0.1 which perfectly matches the comparative measurement of the evaporated Ag film on the QCM presented above. Grazing angle measurements show little difference in the intensity between the two components as compared to normal emission after complete oxidation. The investigated AgO surface is therefore at least homogeneous within the analysis depth of XPS ($\sim$5 nm). We understand the double peak O $1s$ structure with a chemical shift of 2.9 eV as a characteristic feature of AgO.

The oxidation reaction by ECR plasma treatment differs from the reaction caused by a free radical source as used by Tjeng *et al.*[7] due to the presence of ions in the ECR plasma. Therefore, the presence of the ions is a necessity for producing AgO. We would like to stress that no traces of C where measured, excluding therefore contributions to the oxygen signal from CO species. An identical chemical shift between two O $1s$ components as in our measurements was observed by Boronin *et al.*[27] In their work, they interpret the higher BE component to be due to adsorption of exited oxygen species from the plasma on the Ag_2O surface. They understand this peak as a adsorbate species because it vanishes by dosing the surface with 10^8 L of ethylene at 125 °C. However, Tanaka *et al.*[26] have shown by TDS experiments that dosing of AgO with ethylene leads to a bulk reduction of AgO to Ag_2O. Furthermore, over 100 °C AgO starts to decompose into Ag_2O. Therefore, the loss of the higher BE component might as well be due to a reduction of a bulk oxide species different from Ag_2O. As revealed by grazing angle measurements, we can safely exclude in our case that the higher binding energy component is due to adsorbed oxygen at the surface. We further exclude that the higher BE O $1s$ component is due to a mixture of atomic subsurface oxygen and hydroxyl groups as suggested by Weaver *et al.*[9] and Hoflund *et al.*[8] For early stages of the oxidation the lower BE component dominates the spectra. If the higher BE O $1s$ component arises from hydroxyl groups, one would expect that this peak dominates the spectra in an initial phase as the hydrogen content is highest after ignition of the plasma due to desorption of the chamber walls and gas system. Subsurface contributions should be build up before oxygen diffuses into the bulk and would therefore lead to a dominant higher BE component for lower plasma exposure times. This is in contradiction to our observations.

As mentioned above, the oxygen sites in AgO are structurally equivalent and therefore the two peaks cannot be explained from different local structures. In a theoretical work on AgO of Park *et al.*[10] it is suggested, that a large number of holes exist on the oxygen sites. They suggest that silver is present as Ag^+ and Ag^{2+} valences rather than as Ag^+ and Ag^{3+} and consequently, there must exist an considerable amount of oxygen with -1 valency. In a charge transfer model, a negative peak shift in BE for the element with higher electronegativity is expected. For most oxides, the oxygen BE shows a negative peak shift compared to the BE of the free molecule. The shift scales with the valency of the oxygen. In Ag_2O the oxygen atom is present as O^{2-}. As seen in the measurements of Tjeng *et al.*[7] an atom in this configuration shows a BE around 529 eV. As the lower BE O $1s$ component of our measurements lies close to 529 eV, we understand this peak to reflect essentially a -2 valency. The higher BE O $1s$ component at 531.5 eV shows a remarkably smaller shift and a distinct broadening compared to the free molecule and therefore the charge transfer, respectively, the valency must be different. For O^-, such a behavior is expected. The increased peak width indicates a significantly shorter lifetime of the particular state.

Mixed valences can be understood as the fluctuation of the valence state of an atom, e.g., where a valence electron hops between neighboring atoms. Separate binding energy peaks are therefore possible for atoms with different oxidation states in structurally equivalent sites.[28] Kohn *et al.*[29] have theoretically shown, that the observation of the phenomena is not related to the characteristic time of the photoemission process. They showed that a double peak structure can be observed for $U \gg V$ where U is the interaction energy of the electrons on the same nucleus and V is a coupling energy describing the transition between the two electronic configurations. Detailed theoretical discussion of the phenomena can be found in the given reference. We understand the presented results as the manifestation of a $-1/-2$ valency fluctuation on the structurally equivalent O sites. As the electrostatic screening of the other electrons in Ag is considerably higher, the manifestation of the mixed valency as resolvable peaks on the localized $4d$ levels of Ag cannot be expected with the present setup. It rather manifests itself as a broadening of the signal which cannot be resolved from the broadening due to signal components which arise from different local structures around the inequivalent Ag sites.

C. Ultraviolet photoelectron spectroscopy

Figure 4 shows the UPS spectra measured in normal emission (i.e., at the Γ point) for clean Ag(110) and after 30 min of oxidation. (Note, that the produced oxide is not a single crystal.) Figure 4(b) shows the region around E_F. For Ag_2O an electronic gap of 1 eV was found by Tjeng *et al.*[7] We find a gap of 1.09 eV for an intermediate oxidation step while for long oxidations a gap of 0.52 eV was found. We define the gap as the intersection of a linear fit in the background region before the gap and in the edge of the occupied states to E_F. The closing of the gap with ongoing oxidation

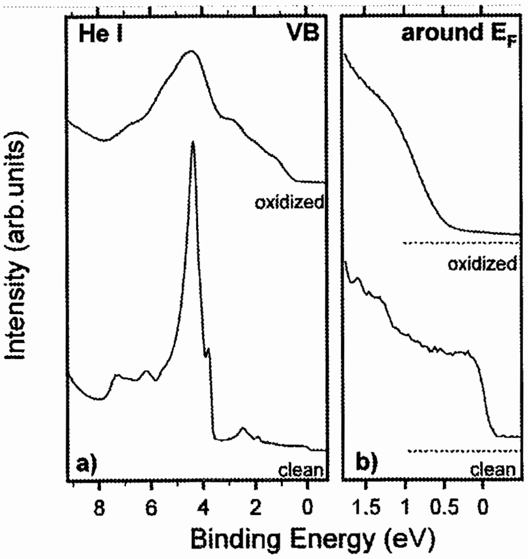

FIG. 4. Valence band spectra measured with HeI radiation at normal emission. (a) Clean and oxidized Ag(110) surface. (b) Shows the Fermi edges for the corresponding measurements. The top of the valenceband of the oxidized sample is located 0.52 eV below the Fermi level.

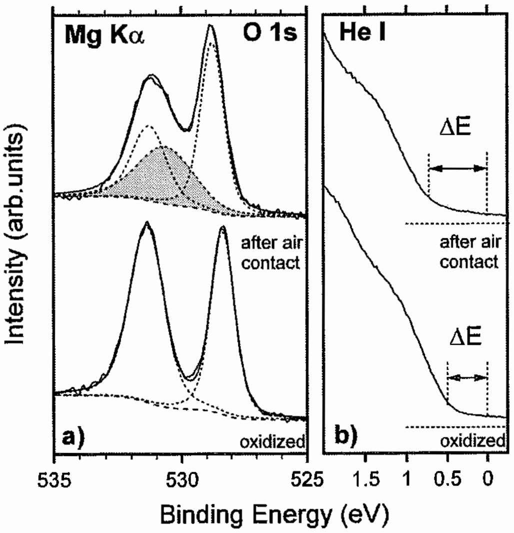

FIG. 5. O 1s signal of a oxidized 1 μm Ag film on Au. (a) O 1s XPS spectra after oxidation and exposure to ambient atmosphere for 17 h. (b) Respective UPS spectra around E_F. The gray shaded area indicates contributions from carbon contaminations. The gap in the UPS spectra increases from 0.5 to 0.72 eV after the contact with air.

corroborates the assumption of oxygen acting as a dopant, as suggested in the model by Park *et al.*[10]

D. Stability

The question of stability of AgO surfaces was addressed by exposing them for prolonged periods to UHV conditions, to ambient atmosphere and to x-ray radiation. These experiments where motivated to understand the behavior of the produced surface exposed to conditions comparable to AgO powder samples transferred to UHV conditions.

After 20 h in UHV at RT, the surface did not show any variations in composition and therefore can be considered stable in UHV for our measurements. The results after contact to ambient atmosphere are presented in Figs. 5(a) (XPS) and 5(b) (UPS). The higher BE O 1s component is strongly reduced while C contaminations lead to multiple O 1s components around 529.5 eV similar to the ones seen by Hoflund *et al.*[8] indicated by a broad, gray shaded peak in Fig. 5(a). Along with the reduction of the higher BE O 1s signal, also a shift of the lower BE signal to higher BE is observed. The respective UPS spectra shown in the Fig. 5(b) reveal an opening of the gap by 0.2 to 0.72 eV. Such a behavior is expected for the surface decomposition of AgO into Ag_2O, the more stable and insulating oxide due to contact with air. These findings lead us to the assumption that AgO powder samples exposed to air already decompose at the surface before any measurement can be performed. Therefore, even if the bulk sample is still AgO in nature, the near surface region within the analysis depth of PES is altered in a way that the gained data are not characteristic for the system. Also, the always present carbon contaminations in powder samples lead to additional O 1s contributions, making interpretation of the results a very difficult and ambiguous task. Ar^+ sputtering does not recover the original AgO surface as the sputtering process itself leads to decomposition of AgO. We observed a degeneration of the oxide under long term x-ray exposure ($P=240$ W). The higher BE signal decreased about 10% compared to the lower binding energy component after 7 h of x-ray exposure. As such a behavior can be observed also with the monochromatic source it is clearly not only related to IR radiation of the x-ray source. The elimination of the higher BE peak indicates a decomposition to the more stable Ag_2O. As our measurements do not demand such extensive radiation exposure, the presented results are not affected by stability issues. Nevertheless, one needs to be aware that PES measurements on AgO can be affected by radiation exposure and demand an *in situ* preparation of the oxide.

IV. DISCUSSION AND SUMMARY

In this work, we presented PES data of *in situ* prepared AgO by ECR plasma treatment at room temperature. To our knowledge, there are no comparable measurements in literature based on *in situ* prepared AgO. The PES spectra exhibit a double peak structure with an BE difference of 2.9 eV. We interpret this double peak structure as a characteristic feature of AgO due to a mixed valence state of the structurally equivalent oxygen atoms. Park *et al.*[10] suggested that Ag atoms are present in a Ag^+ and Ag^{2+} valency rather than Ag^+ and Ag^{3+} as a consequence of e^- holes on the oxygen sites. Therefore, there exist oxygen sites which do exhibit -1 and -2 valences and our measurements do represent this two component.

ACKNOWLEDGMENTS

Skillful technical assistance was provided by R. Schmid, E. Mooser, O. Raetzo, Ch. Neururer, and F. Bourqui. This work was supported by the Swiss National Science Foundation.

[1] R.A. Van Santen and H.P.C.E. Kuipers, Adv. Catal. **35**, 265 (1987).

[2] A.J. Nagy, G. Mestl, and R. Schlögl, J. Low Temp. Phys. **188**, 58 (1999).

[3] G. Schön, Acta Chem. Scand. **27**, 2623 (1973).

[4] J.S. Hammond, S.W. Gaarestroom, and N. Winograd, Anal. Chem. **47**, 2193 (1975).

[5] R.C. Ross, R. Sherman, and R.A. Bunger, Sol. Energy Mater. **19**, 55 (1989).

[6] M. Bowker, Surf. Sci. Lett. **155**, L276 (1985).

[7] L.H. Tjeng, M.B.J. Meinders, J. van Elp, J. Ghijsen, G.A. Sawatzky, and R.L. Johnson, Phys. Rev. B **41**, 3190 (1990).

[8] G.B. Hoflund, Z.F. Hazos, and G.N. Salaita, Phys. Rev. B **62**, 11 126 (2000).

[9] J.F. Weaver and G.B. Hoflund, J. Phys. Chem. **98**, 8519 (1994).

[10] K.T. Park, D.L. Novikov, V.A. Gubanov, and A.J. Freeman, Phys. Rev. B **49**, 4425 (1994).

[11] A. Deb and A.K. Chatterjee, J. Phys. (France) **10**, 11 719 (1998).

[12] M.T. Czyżyk, R.A. de Groot, G. Dalba, P. Fornasini, A. Kisiel, F. Rocca, and E. Burattini, Phys. Rev. B **39**, 9831 (1989).

[13] P. Villars and L. D. Calvert, *Pearson's Handbook of Crystallographic Data for Intermetallic Phases* (American Society for Metals, Metals Park, 1985), Vol. 1.

[14] E. Farhat and S. Robin-Kandare, Thin Solid Films **23**, 315 (1974).

[15] E. Farhat, A. Donnadieu, and J. Robin, Thin Solid Films **29**, 319 (1975).

[16] E. Farhat, A. Donnadieu, and J. Robin, Thin Solid Films **30**, 83 (1975).

[17] R.A. Outlaw, D. Wu, M.R. Davidson, and G.B. Hoflund, J. Vac. Sci. Technol. A **10**, 1497 (1992).

[18] A. Grill, *Cold Plasma in Materials Fabrication* (IEEE Press, New York, 1993).

[19] B. Chapman, *Glow Discharge Processes* (Wiley and Sons, New York, 1980).

[20] J.E. Klemberg-Spicher, O.M. Küttel, L. Martinu, and M.R. Wertheimer, Thin Solid Films **193/194**, 965 (1990).

[21] N. N. Greenwood and A. Earnshaw, *Chemistry of the Elements*, 2nd ed. (Butterworth, London, 1997).

[22] J. Bohdansky, J. Roth, and H.L. Bay, J. Appl. Phys. **51**, 2861 (1980).

[23] G. Carter and D.G. Armour, Thin Solid Films **80**, 13 (1981).

[24] J. J. Yeh and I. Lindau, At. Data Nucl. Data Tables **32**, (1985).

[25] P. Ruffieux, P. Schwaller, O. Gröning, L. Schlapbach, P. Gröning, Q.C. Herd, D. Funnemann, and J. Westermann, Rev. Sci. Instrum. **71**, 3634 (2000).

[26] S. Tanaka and T. Yamashina, J. Catal. **40**, 140 (1975).

[27] A.I. Boronin, S.V. Koscheev, K.T. Murzakhmetov, V.I. Avdeev, and G.M. Zhidomirov, Astron. Astrophys., Suppl. Ser. **165**, 9 (2000).

[28] W. L. Jolly, C. R. Brundle, and A. D. Baker, *Electron Spectroscopy: Theory, Techniques and Applications* (Academic, London, 1977), Vol. 1.

[29] W. Kohn and T.K. Ledd, Philos. Mag. **45**, 313 (1982).